

Theoretical insights into the trends in molecular properties of HCY, HSiY and HGeY molecules where Y = N, P, As

Fariba Nazari · Narjes Ansari

Received: 27 June 2009 / Accepted: 16 September 2009 / Published online: 19 November 2009
© Springer-Verlag 2009

Abstract To obtain insights into the factors that govern the analogy between HCN and its isostructures, HXY where X = C, Si, Ge and Y = N, P, As, the electronic and structural properties of these species in ground, cationic and anionic states at the QCISD, MP2 and B3LYP levels with 6-311++G** basis set and the first excited state with TD-B3LYP method have been presented. The results suggest that there are some correlations between structural and thermodynamic properties of the smallest member of this group (HCN) and heavier congeners. The results of computation at these levels also predict the stability of HCAs in the ground state and HCN, HSiN and HGeN in the cationic state from the energetic point of view. Molecular electrostatic potential map inspection shows that in HXN species nucleophilic region positions on N atom but in HXP and HXAs molecules by increasing the size of central atom nucleophilic region shifts from region near X atom toward terminal atom. Finally, the nature of bonds of HXY molecules are systematically studied through atoms in molecules (AIM) and natural bond orbital analyses (NBO).

Keywords AIM · B3LYP · Dual descriptor · HCN · MESP · MP2 · NBO · QCISD · TD-B3LYP


Introduction

A major reason for the widespread interest in the study of stable compounds with multiple bonds between heavier main group elements (valence electrons of principal quantum number ≥ 3) is that the frequent new findings continue to challenge widely accepted rules of bonding [1]. Especially the so-called double bond rule [2–4] which relates to the supposed inability of elements of principal quantum number ≥ 3 to form multiple bonds. However, due to the detection of the heavy elements in the interstellar medium and after discovery of the first phosphoalkyne [5] (HCP) in 1961 renewed attention has been given to the gas phase chemistry of heavy elements such as: silicon, germanium, nitrogen, phosphorous and arsenic compounds by analogy with the carbon chemistry. Hydrogen cyanide and hydrogen isocyanide are basic chemical compounds of great importance for inorganic and organic chemistry. They were detected in interstellar clouds and a number of comets, including the Hale–Bopp comet [6, 7]. Furthermore, the identification of $\text{Si}\equiv\text{N}$ in the interstellar medium [8] gives the first evidence of a link between the interstellar chemistry of silicon and that of nitrogen. There exists also a reliable spectroscopic constant on a series of related compounds (HSiN) [9].

After discovery of the HCP [5], in 1981 the first stable compound involving a heavier element (tBuCP) was synthesized [10]. Mes*CA_s (Mes*=2,4,6-tri-tert-butylphenyl) is only one example of a stable arsaalkyne that was structurally characterized in 1986 [11]. The thermal stability of Mes*CA_s is mainly due to the bulky Mes* group. A further stabilizing effect may be the interaction of the aryl π system with the $\text{C}\equiv\text{As}$ triple bond, as found in anionic phosphoalkynes. The only other known arsaalkyne, CH_3CA_s [12], is unstable at room temperature and the parent compound, HCAs, is still unknown.

Electronic supplementary material The online version of this article (doi:10.1007/s00894-009-0600-4) contains supplementary material, which is available to authorized users.

F. Nazari (✉) · N. Ansari
Faculty of Chemistry,
Institute for Advanced Studies in Basic Sciences (IASBS),
5195-1159, Zanjan 45195, Iran
e-mail: nazari@iasbs.ac.ir

Table 1 Optimized structural parameters and electron density at bond critical point from AIM analysis at MP2, B3LYP and QCISD levels for HGeY group


M	MS	R1		R2		A1		ρ1		ρ2		R1		R2		A1		ρ1		ρ2	
		R1	R2	A1	ρ1	ρ2	R1	R2	A1	ρ1	ρ2	R1	R2	A1	ρ1	ρ2					
HGeN	G	1.53	1.70	180.00	0.13	0.17	1.52	1.64	180.00	0.14	0.20	1.53	1.66	180.00	0.13	0.18					
	A	1.62	1.84	95.39	0.11	0.13	1.65	1.77	99.32	0.10	0.16	1.64	1.78	100.97	0.10	0.15					
	C	1.51	1.75	180.00	0.14	0.17	1.53	1.72	180.00	0.14	0.18	1.53	1.75	174.83	0.14	0.12					
	ES	-	-	-	-	-	1.61	1.84	100.37	0.11	0.14	-	-	-	-	-					
HGeP	G	1.52	2.04	180.00	0.13	0.12	1.52	2.01	180.00	0.14	0.13	1.53	2.03	180.00	0.13	0.12					
	A	1.61	2.16	99.51	0.11	0.11	1.63	2.20	99.54	0.11	0.11	1.62	2.20	98.81	0.11	0.10					
	C	1.52	2.11	180.00	0.14	0.12	1.53	2.10	180.00	0.14	0.12	1.52	2.11	180.00	0.14	0.12					
	ES	-	-	-	-	-	1.60	2.33	96.25	0.11	0.09	-	-	-	-	-					
HGeAs	G	1.53	2.15	180.00	0.13	0.10	1.53	2.11	180.00	0.14	0.08	1.53	2.14	180.00	0.13	0.10					
	A	1.61	2.28	98.28	0.11	0.10	1.62	2.31	98.36	0.11	0.09	1.62	2.33	97.60	0.11	0.09					
	C	1.52	2.21	180.00	0.14	0.10	1.53	2.21	180.00	0.14	0.10	1.53	2.23	180.00	0.14	0.10					
	ES	-	-	-	-	-	1.56	2.28	125.14	0.13	0.09	-	-	-	-	-					

M, MS, G, A, C and ES stand for molecule, molecular state, ground, anionic, cationic and excited states, respectively.

Although the characteristics of compounds with $C\equiv N$ triple bonds (nitriles) have been well-known for a very long time, this is not true for the corresponding phosphorus-, arsenic-, silicon- and germanium- containing analogues and the capacity of second- and third-row atoms to form multiple

bonds has been an intriguing problem in chemistry [13]. Yanez et al. have worked on the characterization of the intrinsic reactivity of low-stability compounds, which contain second-, third-, and fourth-row atoms such as P, As, Si, Ge, and Sn [14–17]. Along this line for the first time, quantitative information, from both the experimental and the theoretical point of view, on the gas-phase acidity of HCP, CH_3CP , HCAs, and CH_3CAs have been reported in 2002 [13].

Table 2 Nature and number of σ and π bonds of $X\equiv Y$ (BD-Nature), and existing lone pair on atoms of anionic state (LP_A) from NBO analyses for ground (G), cationic (C) and anionic (A) states

X≡Y	BD-Nature			
	G	C	A	LP_A
CN	2c-6e	2c-5e	2c-6e	H (1e)
	2 π , 1 σ	1.5 π , 1 σ	2 π , 1 σ	-
CP	2c-6e	2c-5e	2c-5e	C (1e)
	2 π , 1 σ	1.5 π , 1 σ	1.5 π , 1 σ	P (1e)
CAs	2c-6e	2c-5e	2c-5e	C (1e)
	2 π , 1 σ	1.5 π , 1 σ	1 π , 1.5 σ	As (1e)
SiN	2c-6e	2c-5e	2c-4e	Si (2e)
	2 π , 1 σ	1.5 π , 1 σ	1 π , 1 σ	N (1e)
SiP	2c-6e	2c-5e	2c-5e	Si (2e)
	2 π , 1 σ	1.5 π , 1 σ	1 π , 1 σ	P (1e)
SiAs	2c-6e	2c-5e	2c-4e	Si (2e)
	2 π , 1 σ	1.5 π , 1 σ	1 π , 1 σ	As (1e)
GeN	2c-6e	2c-5e	2c-4e	Ge (2e)
	2 π , 1 σ	1.5 π , 1 σ	1 π , 1 σ	N (1e)
GeP	2c-6e	2c-5e	2c-4e	Ge (2e)
	2 π , 1 σ	1.5 π , 1 σ	1 π , 1 σ	P (1e)
GeAs	2c-6e	2c-5e	2c-4e	Ge (2e)
	2 π , 1 σ	1.5 π , 1 σ	1 π , 1 σ	As (1e)

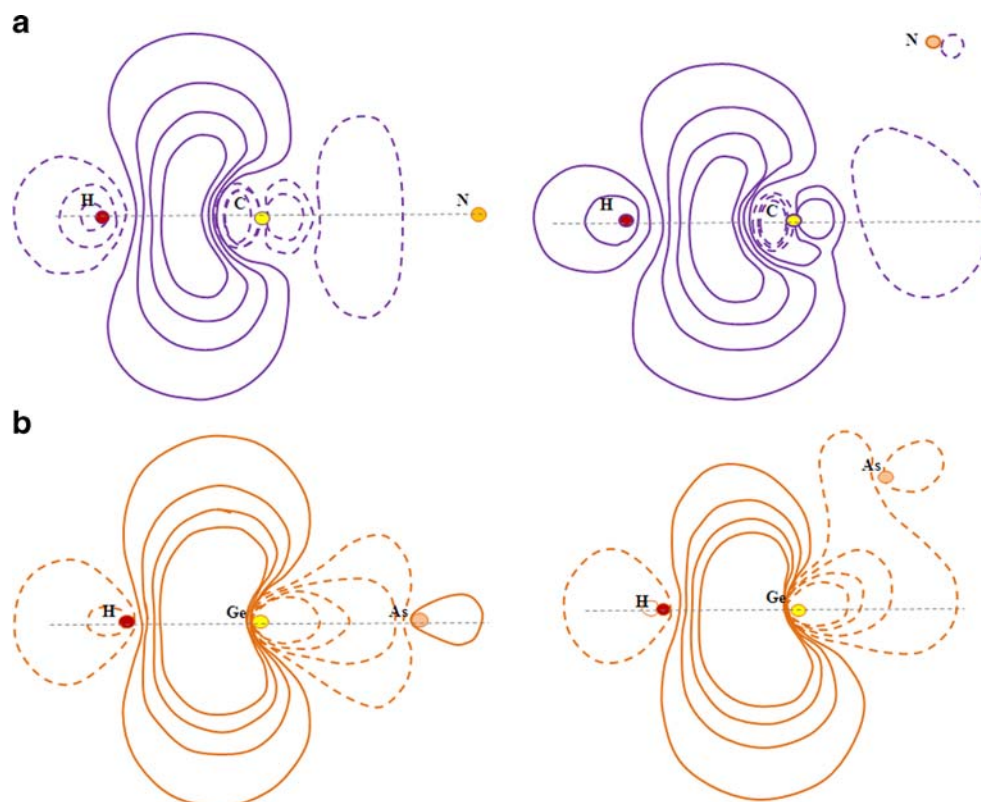
On the other hand, quantum chemistry computations generate increasingly large amounts of data that call for more attention to systematization. Such systematization is facilitated by analysis of electronic wave functions [18]. Modern approaches to analysis of electronic wave functions are the definition of properties such as atomic charges, energies, valencies, bond orders, specialized orbitals, population analysis, and frequencies.

The aim of the present report is to complete description of the properties and some correlations to the presented evidence at the introduction. Such a scope necessarily requires a quantitative study of the HXY molecules with computational quantum chemistry methods and wave function analyses, which are attractive approaches for understanding the structure and bonding in the heavier main group elements and systematization of obtained data.

Computational methods

Geometry optimization for neutral, cationic and anionic states of HXY molecules were performed by using QCISD

Fig. 1 NHOs in ground and first excited states at B3LYP level (a) h_C of HCN molecule, and (b) h_{Ge} of HGeAs molecule



[19], MP2 [20–24] and the density functional theory (DFT) [25, 26] with the B3LYP [27–29] hybrid functional methods, as implemented in Gaussian03 [30] with popular 6-311++G (d,p) basis set [31]. The optimized geometries were characterized by harmonic analysis, and the nature of the stationary points was determined according to the number of negative eigenvalues of the Hessian matrix. Singlet first excited state structures were obtained at the CIS/6-311++G(d,p) [31, 32] and TD-B3LYP/6-311++G(d,p) [31, 33] levels. The same level of theory was also utilized for obtaining the wave functions of all the optimized structures.

The bonding features of all the studied species were analyzed by means of the natural bond orbital (NBO) and

the natural population analyses (NPA) [34, 35]. We have also analyzed the nature of the bonding by using the atoms in molecules (AIM) [36] approach. Reactivity of different atoms in studied molecules are investigated by using molecular electrostatic potential (MESP) [37, 38], Fukui functions (FF) [39, 40] and dual descriptor (Δf) [41]. The FF and Δf were calculated as follows:

$$f_k^+ = q_K(N+1) - q_K(N) \text{ FF for nucleophilic attack} \quad (1)$$

$$f_k^- = q_K(N) - q_K(N-1) \text{ FF for electrophilic attack} \quad (2)$$

$$\Delta f = f^+ - f^- \quad \text{Dual descriptor} \quad (3)$$

$$\Delta f \approx \rho^{LUMO}(r) - \rho^{HOMO}(r) \quad \text{Dual descriptor} \quad (4)$$

where q_k is the electronic population of atom k in a molecule and $\rho(r)$ is the electron density.

Results and discussions

Optimized structural parameters for the four molecular states and electron density at bond critical points from AIM analysis along with the available experimental data are depicted in Table 1 for HGeY group and in (Supplementary

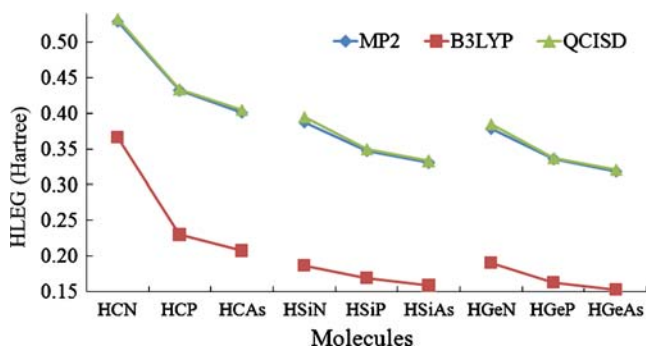


Fig. 2 Stability trends of the optimized HXY molecules in ground (G) state, according to their HOMO-LUMO energy gaps'

material Table 1S) for the HCY and HSiY groups. Good agreement is found between the experimental and the calculated data. Except anionic HCN, all anionic and first excited states of studied molecules are bent. Except for cationic HSiN, HSiP and HGeN at QCISD level all ground and cationic structures are linear. These observations are confirmed by NBO analyses. These analyses show that in cationic and anionic forms the bond order of $X\equiv Y$ bonds reduces and as a result the bond lengths increase. There are, in addition, lone pair molecular orbitals on central atoms of anionic forms and these are the cause of deviation from linearity according to Walsh's rule [42–45]. All H-X bonds have two center-two electron (2c-2e) character. Details of the NBO analyses for $X\equiv Y$ bonds are given in Table 2. Except for minor difference in anionic $\text{Ge}\equiv\text{P}$ and $\text{Ge}\equiv\text{As}$ which have different distorted triple bond, the NBO results of the other cases are the same for three levels of computation. First excited state bent structures can be explained by bending of natural hybrid orbitals (NHOs) from line of centers in comparison with linear ground state structures. As an example NHOs of carbon atom (h_{C}) of HCN molecule and germanium atom (h_{Ge}) of HGeAs molecule in ground and first excited states are visualized by NBOView [46] and depicted in Fig. 1.

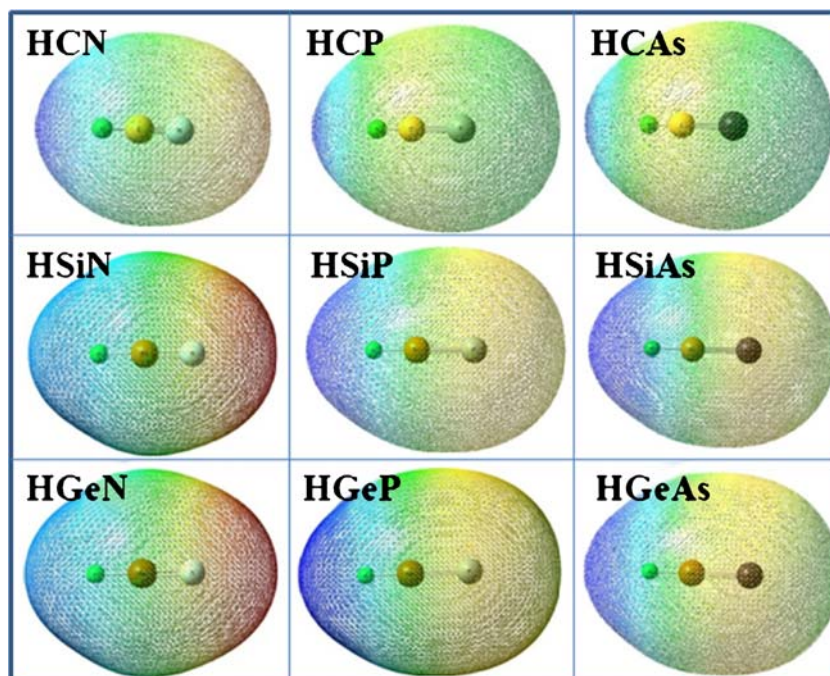
Molecular properties

For candidate molecules in ground, first excited, cationic and anionic states different molecular properties (e.g., ionization potential (IP), electron affinity (EA), polarizability, dipole moment (μ), and HOMO-LUMO energy gap

(HLEG) are calculated. The HLEG is a sensitive quantity to probe the stability [47]. In accordance with this quantity the stability trends of optimized HXY molecules with post Hartree-Fock (QCISD and MP2) and B3LYP methods are depicted in (Fig. 2) for ground state and for first excited, cationic and anionic states in (Supplementary material Fig. 1S). The existing experimental data for HCN [6, 7, 48], HCP [5, 49], HSiN [9] and HCP^+ cation radical [50] species confirm the stability of these species in their ground and cationic states. The stability trends of optimized HXY molecules in their ground, cationic, anionic, and first excited states derived from the HLEG show that the HLEG of some of HXY molecules are in the range of the calculated values of HLEG of stable HCN, HCP, HSiN, and HCP^+ species. It can be concluded that HCAs in its ground state and HCN, HSiN, and HGeN species in their cationic states can exist from the energetic point of view at these levels of computation.

The trends of variation of IP, EA, polarizability and μ are given in (Supplementary material Figs. 2aS–2hS). Calculated vertical and adiabatic IPs and EAs and those obtained from Koopman's theorem (KT) for HCY, HSiY and HGeY species are compared in (Supplementary material Figs. 2aS–2fS). Although the calculated values of IPs and EAs from these three approaches have the same trends the corresponding values are different. Vertical and adiabatic IPs are the same for all HXY species while, except HCN, calculated vertical and adiabatic EAs have different values. A geometric comparison of ground, cationic and anionic states shows that optimized ground and cationic states have linear structures but optimized anionic states have bent

Fig. 3 Electrostatic potential plots of HXY molecules in the ground state mapped onto electron density values with isodensity values of 0.00004 a.u.



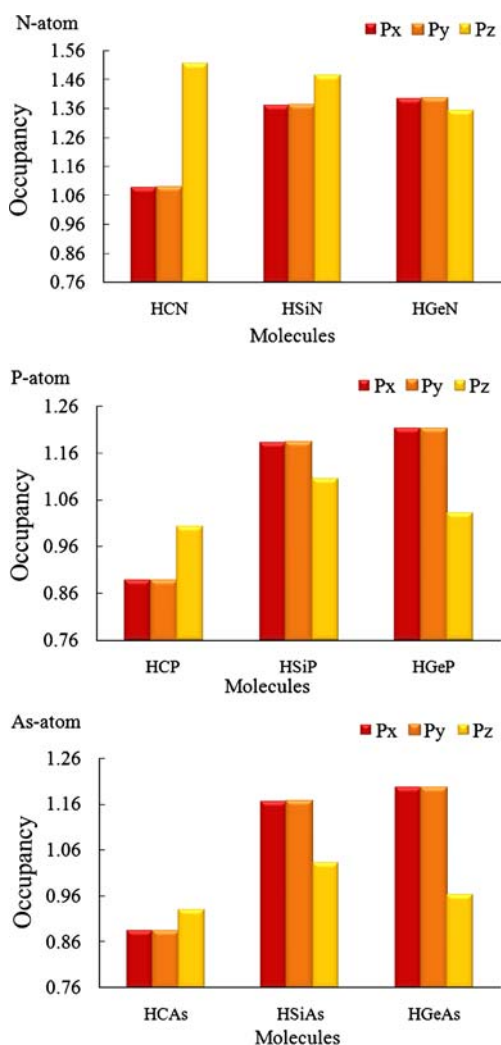


Fig. 4 Occupancy of valance NAOs for terminal Y (N, P, As) atoms in ground state of HXY species

structures. As pointed out in the literature [51] different optimized geometrical structures of neutral and anionic states are one of the reasons for the difference in adiabatic and vertical EA values. Inspections in the calculated

properties, in addition, show that, except for HGeY group with QCISD method, by increasing the size of molecules the IPs decrease in ground and first excited states but the polarizabilities have reverse trends.

An assessment of data in (Supplementary material Fig. 2gS) show that ground states of HXN molecules have dipole moment greater than 2.5 Debye. By substitution of N with P and As atoms, dipole moment of HXP and HXAs molecules decreases in comparison with HXN molecules. In the structures with $\mu \geq 2.5$ D the electronegativity difference of Y and X atoms is positive ($\chi_Y - \chi_X > 0$). There is a good agreement between computed dipole moment for HCN (3.02, 2.95, 3.05, D) and HCP (0.31, 0.30, 0.36 D) at QCISD, MP2 and B3LYP levels, respectively and reported experimental values of HCN (2.99 D) [52] and HCP (0.39 D) [53]. On the other way, neutral molecules with $\mu \geq 2.5$ D can form dipole-bound anions, unless there are atoms or functional groups occupying the region of space where the excess electron would otherwise be bound [54]. In dipole-bound anions, electrons bind to polar molecules and this issue is reported in many theoretical studies [55–57]. Anions may have negative electron affinity (*e.g.*, HCN) which constituted dipole-bound anions. However, some molecules with $\mu \geq 2.5$ D have positive electron affinity (*e.g.*, HSiN, HGeN). Silicon and germanium atoms in HSiN and HGeN molecules provide the region of space where the excess electron would be bound.

Atomic charges for H, X, and Y atoms can be calculated by different approaches. AIM, Mulikan and NPA are among them. The NPA and the AIM charges for H, X, and Y atoms in different molecular states are compared. Though the AIM and the NPA charges have different values, they follow similar trends with the exception of some minor cases. These values transform to information about chemistry and, especially, chemical reactivity. Among different reactivity indicators, FF successfully predicts relative site reactivity for most chemical systems. It also is emphasized that the FF depends highly on population analysis schemes

Table 3 Classification the nature of bonds according to Bader et al. (L), Cremer et al. (M), Esspinosa et al. (N) from AIM analyses, % covalence character (O) and % ionic character (Q) of bonds from NBO analyses at QCISD level for ground states. Sh, CS and IM are representative of Share, Close Shell and Intermediate interactions, respectively

Molecule	H–X					X≡Y				
	L	M	N	O	Q	L	M	N	O	Q
HCN	Sh	Sh	Sh	78.65	21.35	Sh	Sh	Sh	88.19	11.81
HCP	Sh	Sh	Sh	79.34	20.66	Sh	Sh	Sh	82.37	17.63
HCAs	Sh	Sh	Sh	80.24	19.76	Sh	Sh	Sh	81.39	18.61
HSiN	IM	Sh	IM	85.84	14.16	IM	Sh	IM	62.01	37.99
HSiP	IM	Sh	IM	88.53	11.47	IM	Sh	IM	84.51	15.49
HSiAs	IM	Sh	IM	87.76	12.24	IM	Sh	IM	83.42	16.58
HGeN	Sh	Sh	Sh	87.03	12.97	Sh	Sh	Sh	63.08	36.92
HGeP	IM	Sh	IM	90.34	9.66	Sh	Sh	Sh	81.74	18.26
HGeAs	IM	Sh	IM	89.85	10.15	Sh	Sh	Sh	80.72	19.28

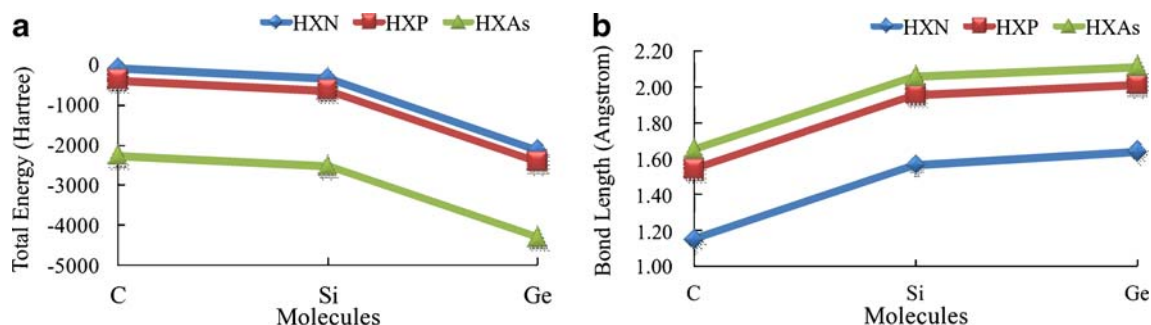


Fig. 5 Comparative diagram (a) energy and (b) X=Y bond length for the ground state of HXY species

[58]. Calculated FF and Δf by using Eqs. 1, 2, 3 at B3LYP level from the AIM and the NPA charges are depicted in Supplementary material (Figs. 3aS–3iS) and (Supplementary material Figs. 4aS–4cS) represent the Δf by using Eq. 4 from B3LYP, MP2, and QCISD densities which are generated and mapped onto electron density using GaussView 4.1 [59] with isodensity setting 0.00004 atomic unit. The surfaces are defined by the 0.002 electrons/bohr³ contour of the molecular electronic density. The color-coded regions on the surfaces describe red as negative and blue as positive region. Analyses the details of figures (Supplementary material Figs. 3aS–3iS) show in some cases there are not agreement between calculated reactivity descriptors (f^+ , f^- , Δf) values from two different charges. As an example, Δf from AIM charges for arsenic atom in HSiAs molecule (Supplementary material Fig. 3fS) is less than zero which means arsenic atom is a nucleophilic region but the prediction with the NPA charges is reverse. Predicted electrophilic and nucleophilic character of a different region by FF and Δf also are not compatible.

Inspection of the (Supplementary material Figs. 4aS–4cS) shows that except for the HCP all the HXP and HXAs groups in the three approaches have the same trends and HXN group have irregular behavior in positioning the $\Delta f < 0$ and $\Delta f > 0$ regions. On the other hand based on these data

one cannot predict the exact position of the nucleophilic and electrophilic regions.

It was pointed out that the MESP is used extensively on qualitative and semi-quantitative levels as a probe for locating the reactive regions in a molecule. For example, by employing MESP contour maps, one can see the spatial regions in which the MESP is negative and to which an electrophile would initially be attracted [37].

Figure 3 represents MESP for HXY molecules in the ground state which are the same in three computational levels. The electrostatic potential plots are generated with the same parameters as the Δf maps. In HXN species the nucleophilic region positions on N atom but in HXP and HXAs molecules by increasing the size of central atom the nucleophilic region shifts from the region near X atom toward terminal atom. In addition, analyses of the NAOs occupancy of the valance orbitals can be used as evidence for the reactivity of HXY species. At B3LYP level of computation variation of the occupancy of valance orbitals of Y atoms is depicted in (Fig. 4). Comparison of these diagrams with MESP contour maps reveals that by increasing the nucleophilic character of terminal atom the occupancy of the valance orbitals of associated atom, except p_z orbital, increases too.

The NBO and AIM analyses results for nature of H-X and X=Y bonds at QCISD level just for ground state are

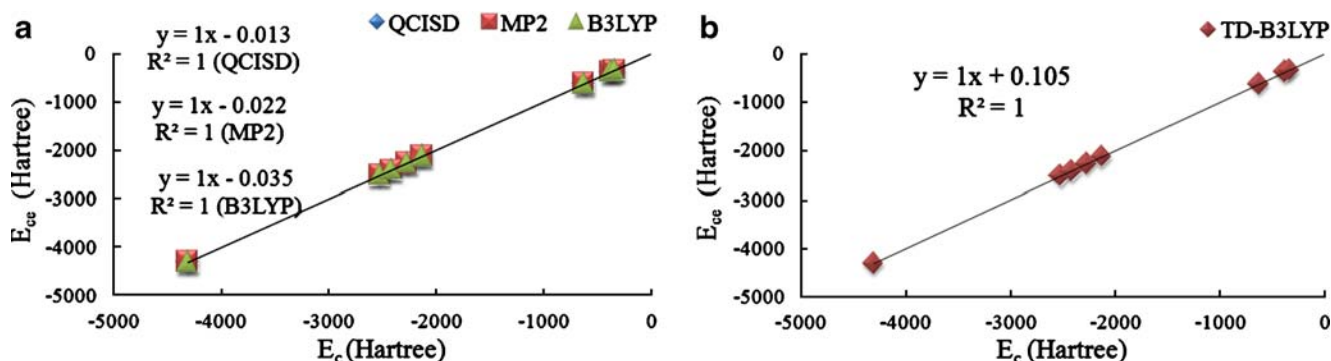


Fig. 6 Correlation between total energy at QCISD, MP2, and B3LYP level (E_c) and calculated total energy from Eq. 5 (E_{cc}) for HXY species in ground (a) and first excited (b) states (Hartree)

Table 4 Error percentages for calculated thermodynamic parameters from Eq. 5 in ground states at three levels

Molecule	QCISD			MP2			B3LYP		
	E	H	G	E	H	G	E	H	G
HCP	0.0087	0.0087	0.0091	0.0056	0.0056	0.0060	0.0010	0.0010	0.0014
HCA _s	-0.0004	-0.0004	-0.0002	-0.0008	-0.0007	-0.0006	-0.0007	-0.0007	-0.0006
HSiN	-0.0216	-0.0219	-0.0208	-0.0216	-0.0217	-0.0211	-0.0267	-0.0269	-0.0261
HSiP	0.0056	0.0054	0.0063	0.0011	0.0010	0.0016	0.0024	0.0023	0.0029
HSiAs	0.0009	0.0008	0.0011	-0.0002	-0.0002	0.0000	0.0002	0.0001	0.0004
HGeN	-0.0054	-0.0055	-0.0052	-0.0051	-0.0051	-0.0050	-0.0060	-0.0061	-0.0059
HGeP	0.0005	0.0004	0.0007	-0.0005	-0.0005	-0.0003	-0.0002	-0.0002	0.0000
HGeAs	0.0000	0.0000	0.0002	-0.0006	-0.0006	-0.0005	-0.0003	-0.0003	-0.0002

E, H, and G stand for total electronic energy, enthalpy, and Gibbs free energy.

given in Table 3 and in Supplementary material, Table 2S at QCISD, MP2 and B3LYP levels for remaining states. Results for nature of bonds are given according to Cremer et al. [60], Esspinosa et al. [61] and Bader et al. [62] concepts. NBO results for nature of bonds are taken from standalone GENNBO program [63]. Most of the bonds according to these concepts have dominated covalent character, but none of these strategies have been found to be universal in their application.

Data systematization

Investigating the correlation between the properties of studied molecules, relationship between structural parameters and thermodynamic properties of the smallest member of this group (HCN) with the same properties in heavier congeners of these series have been formulated. These formulations are illustrated in section i and ii. In section i, a relationship between the thermodynamic properties of HXY molecules and thermodynamic properties of HCN ($Z_{HXY}=f(Z_{HCN})$) is denoted. The same as section i a correlation between bond lengths of HXY molecules as a function of bond lengths of HCN molecule, ($BL_{HXY}=f(BL_{HCN})$) is symbolized.

i. $Z_{HXY} = f(Z_{HCN})$

Obtaining the correlation between thermodynamic properties of HXY molecules and thermodynamic properties of HCN molecule, as an example, computed total energies of HXY molecules in the ground state at B3LYP/6-311++G** level are compared in (Fig. 5a). Assessment of this figure reveals that energy variation in these molecules have a regularity. Based on this regularity Eq. 5 is proposed for calculating the total energy, enthalpy and Gibbs free energy in ground, first excited, anionic, and cationic states of HCN isostructures. By using this equation, calculation is done only on HCN molecule in these states along with computation on isolated atomic species of heavier elements of carbon and nitrogen groups. These equations are:

$$Z_{HXY}^{\mp 0 \uparrow} = Z_{HCN}^{\mp 0 \uparrow} + (E_X^{\mp 0 \uparrow} - E_C^{\mp 0 \uparrow}) + (E_Y^{\mp 0 \uparrow} - E_N^{\mp 0 \uparrow}) - S_{HXY}^{\mp 0 \uparrow} \tag{5}$$

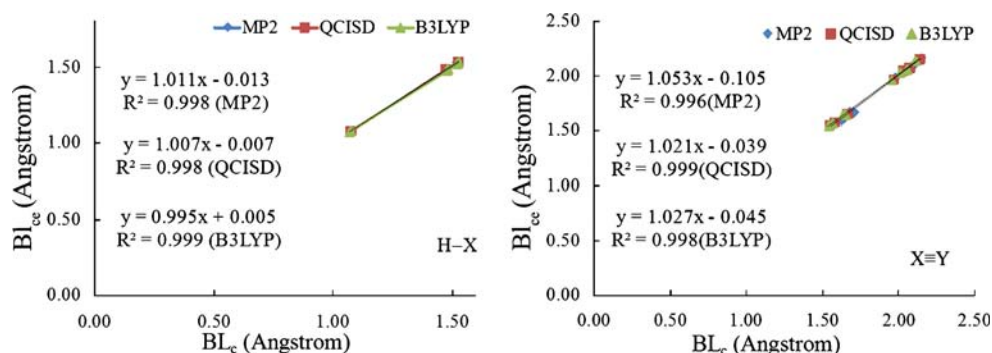
$$S_{HXY}^{\mp 0 \uparrow} = W_{X \neq C}^{\mp 0 \uparrow} + W_{Y \neq N}^{\mp 0 \uparrow}, W = V/E_{en} - 1 \tag{6}$$

In Eq. 5 $Z_{HXY}^{\pm 0 \uparrow}$ is the representative of total energy, enthalpy or Gibbs free energy in ground (°), first excited (↑), anionic (-) and cationic (+) states. E_x and E_y in Eq. 5 are total

Table 5 Definition of a and b parameters of Eq. 8

	H-X	X≡Y
a	$\frac{5}{2} + \frac{5}{100} + \gamma, \gamma = \begin{cases} 0 & \text{for Si} \\ \frac{20}{100} & \text{for Ge} \end{cases}$	$\frac{5}{2} + \frac{5}{100} + \gamma, \gamma = \begin{cases} \frac{5}{100} & \text{for Si} \\ \frac{45}{100} & \text{for Ge} \end{cases}$
b	$\frac{6}{100}$	$\frac{5}{2} + \frac{5}{100} + \gamma, \gamma = \begin{cases} -\frac{10}{100} & \text{for P} \\ \frac{45}{100} & \text{for As} \end{cases}$

Fig. 7 Correlation between calculated bond lengths from Eq. 7 (BL_{cc}) and optimized bond lengths at QCISD, MP2, and B3LYP levels (BL_c) for H-X and X≡Y bonds in ground states (unit is Å)



energies of isolated X and Y atoms which can be calculated in the same computational level as HCN molecule. E_{en} and V are electron–nuclear attraction and potential energy terms of isolated X and Y atomic species, respectively. Figure 6 exemplifies the correlation between calculated total energy from Eq. 5 and computed total energy at three levels in the ground state and first excited state only at TD-B3LYP level. The error percentages for calculate thermodynamic parameters in ground states at three levels are listed in Table 4 and for other states are given in Supplementary material, Tables 3S. Inspection of the data shows that the $S_{HXY}^{\pm\sigma\uparrow}$ parameter can be held as the representative of the effect of interactions between H, X, and Y atoms in HXY molecules.

ii. $BL_{HXY} = f(BL_{HCN})$

The same as section i but for the correlation between bond lengths of HXY molecules with the bond lengths of HCN molecule, (Fig. 5b) exemplifies the variation of X≡Y bond length in HXY molecules in the ground state. According to bond lengths variation in HXY molecules the correlation between bond lengths of smallest member of this group and atomic total energies of constituent isolated atoms and bond lengths of H-X and X≡Y bonds in HXY molecules are given in Eq. 7.

$$BL_{HXY}^{\mp0\uparrow} = BL_{HCN}^{\mp0\uparrow} + \frac{1}{(E_X^{\mp0\uparrow} - E_C^{\mp0\uparrow})} + \frac{1}{(E_Y^{\mp0\uparrow} - E_N^{\mp0\uparrow})} - U_{HXY}^{\mp0\uparrow} \quad (7)$$

Table 6 Error percentages for calculated bond lengths from Eq. 7 in ground states at three levels and first excited state at TD-B3LYP level

Molecule	QCISD		MP2		B3LYP		TD-B3LYP	
	H-X	X≡Y	H-X	X≡Y	H-X	X≡Y	H-X	X≡Y
HCP	0.01	-0.15	0.18	-0.19	0.03	0.09	-3.25	0.92
HCA _s	-0.02	0.62	0.19	0.82	-0.04	0.54	-3.39	2.20
HSiN	-0.17	0.12	0.11	2.18	0.55	0.03	-0.20	-0.71
HSiP	-0.86	-0.06	-0.79	-0.05	-0.01	0.16	-1.16	4.27
HSiAs	-0.98	0.14	-0.87	0.23	-0.07	0.01	-1.69	6.20
HGeN	0.38	0.67	0.43	2.18	0.27	-0.21	1.88	2.76
HGeP	-0.19	-0.69	-0.29	-0.78	0.01	-0.92	1.28	6.23
HGeAs	-0.13	-0.48	-0.24	-0.51	0.09	-1.04	-1.47	0.04

$$U_{HXY}^{\mp0\uparrow} = aW_{X\neq C}^{\mp0\uparrow} + bW_{Y\neq N}^{\mp0\uparrow} \quad (8)$$

where except a and b all parameters in Eqs. 7 and 8 have similar definition to parameters in Eqs. 5 and 6. Definition of a and b parameters are depicted in Table 5. Figure 7 illustrates this correlation for ground state and Table 6 shows the error percentages of the calculated bond lengths from Eq. 7 in comparison with the optimized bond lengths at QCISD, MP2, and B3LYP levels. For other states are given in Supplementary material, Tables 4S.

Inspections of the Table 6 and (Fig. 7) show that except some minor case (cationic HSiN at MP2 level) the H-X and X≡Y bond lengths values which are obtained from Eq. 7 for ground and cationic states are in good agreement with the optimized values at three levels. In some of the anionic and first excited states obtained values from Eq. 7 deviate from the computed values at these three levels. Maximum value of deviation is ~7% and belongs to anionic state. When the HXY species have the same geometry as HCN molecule in different states this correlation works well. This is proven by inspection of the calculated values for cationic and first excited states. On the other hand because the structure of anionic HXY species differ from anionic HCN the error percentage increases.

Conclusions

Currently, the availability of experimental data for the system treated here (except HCN, HCP, and HSiN which

they have good agreement with experimental data) is scarce. This of course makes it difficult to discuss our result in an experimental context and to validate our computational data. As mentioned experimental data exist for HCN, HCP, HSiN, and HCP⁺ species. Stability trends of optimized HXY molecules in their ground states based on the HLEG show that the HLEG of some of HXY molecules is in the range of the HLEG of HCN, HCP, and HSiN species. It can be concluded that molecules like HGeN in the ground state and HCN, HSiN, and HGeN in the cationic state can exist from the energetic point of view at these three levels of computation. Most of the bonds according to wave function analyses have dominated covalent character in all states. Molecular electrostatic potential map inspection shows that in HXN species nucleophilic region positions on N atom but in HXP and HXAs molecules by increasing the size of the central atom nucleophilic region shifts from the region near X atom toward terminal atom.

Electronic structure theory analysis of the heavier congeners of HCN molecule also reveals that there exists a good correlation between structural and thermodynamic properties of the smallest member of this group (HCN) and heavier congeners. It seems that the introduced parameters (*S* and *U*) in Eqs. 5 and 7 besides the HCN parameters are representative of the effect of interactions between H, X, and Y atoms in HXY molecules.

Finally, the comparison of the QCISD, MP2, and B3LYP show that except in minor cases there is a good agreement between the results of these three levels.

Acknowledgments Fariba Nazari thanks the Newcastle University of Australia (Callaghan Campus) for their support for doing the computation during her academic visit.

References

- Dasent WE (1965) Non existent compounds-compounds of low stability. Marcel Dekker, New York
- Kuchta MC, Parkin G (1998) Terminal chalcogenido complexes of Group 13 and 14 elements. *Coord Chem Rev* 176:323–372
- Jutzi P (1975) New element-carbon (p-p) π bonds. *Angew Chem Int Ed Engl* 14:232–245
- Gusel'nikov LE, Nametkin NS (1979) Formation and properties of unstable intermediates containing multiple p.pi.-p.pi. bonded Group 4B metals. *Chem Rev* 79:529–577
- Gier TE (1961) HCP, a unique phosphorus compound. *J Am Chem Soc* 83:1769–1770
- Hirota T, Yamamoto S, Kawaguchi K, Sakamoto A, Ukita N (1999) Observations of HCN, HNC, and NHs in comet Hale-Bopp. *Astrophys J* 520:895–900
- Rodgers SD, Charnley SB (1998) HNC and HCN in comets. *Astrophys J* 501:L227–L230
- Turner BE (1992) Detection of silicon nitride (SiN) in IRC+10216. *Astrophys J* 388:L35–L38
- Maier G, Glatthaar J (1994) Silane nitrile: matrix isolation, adduct with hydrogen. *Angew Chem Int Ed Engl* 33:473–475
- Becker G, Gresser G, Uhl W (1981) Acyl- und Alkyldenphosphane. (XV) 2,2-Dimethylpropylidindiphosphan, eine stabile Verbindung mit einem Phosphoratom der Koordinationszahl 1. *Z Naturforsch* 36b:16–19
- Markl G, Sejpka H (1986) 2-(2, 4, 6-Tri-tert-butylphenyl)-1-arsaethyne- the first compound containing an arsenic-carbon triple bond. *Angew Chem Int Ed Engl* 25:264–264
- Guillemin JC, Lassalle L, Drean P, Wlodarczak G, Demaison J (1994) Synthesis and spectroscopic characterization of ethylidynearsine. *J Am Chem Soc* 116:8930–8936
- Mo O, Yanez M, Guillemin JC, Riague EH, Gal JF, Maria PC, Poliart CD (2002) The gas-phase acidity of HCP, CH₃CP, HCAs, and CH₃CAs: an unexpected enhanced acidity of the methyl group. *chemistry-a European Journal* 8:4919–4924
- Guillemin JC, Decouzon M, Maria PC, Gal JF, Mo O, Yanez M (1997) Gas-phase basicities and acidities of ethyl-, vinyl-, and ethynylarsine. An experimental and theoretical study. *J Phys Chem A* 101:9525–9530
- Mo O, Yanez M, Decouzon M, Gal JF, Maria PC, Guillemin JC (1999) Gas-phase basicity and acidity trends in α , β -unsaturated amines, phosphines, and arsines. *J Am Chem Soc* 121:4653–4663
- Gal JF, Decouzon M, Maria PC, Gonzalez AI, Mo O, Yanez M, Chaouch SE, Guillemin JC (2001) Acidity trends in α , β -Unsaturated alkanes, silanes, germanes, and stannanes. *J Am Chem Soc* 123:6353–6359
- Benidar A, Le Doucen R, Guillemin JC, Mo O, Yanez M (2001) Vibrational spectra, DFT calculations, and assignments of the *syn* and the *gauche* forms of vinylphosphine. *J Mol Spec* 205:252–260
- Cioslowski J (2000) In: Schleyer PvR (ed) Handbook of computational chemistry. Wiley, New York
- Pople JA, Head-Gordon M, Raghavachari K (1987) Quadratic configuration interaction. A general technique for determining electron correlation energies. *J Chem Phys* 87:5968–5975
- Frisch MJ, Head-Gordon M, Pople JA (1990) A direct MP2 gradient method. *Chem Phys Lett* 166:275–280
- Head-Gordon M, Pople JA, Frisch MJ (1988) MP2 energy evaluation by direct methods. *Chem Phys Lett* 153:503–506
- Frisch MJ, Head-Gordon PJA (1990) Semi-direct algorithms for the MP2 energy and gradient. *Chem Phys Lett* 166:281–289
- Head-Gordon , Head-Gordon T (1994) Analytic MP2 frequencies without fifth-order storage, Theory and application to bifurcated hydrogen bonds in the water hexamer. *Chem Phys Lett* 220:122–128
- Saebo S, Almlöf J (1989) Avoiding the integral storage bottleneck in LCAO calculations of electron correlation. *Chem Phys Lett* 154:83–89
- Hohenberg P, Kohn W (1964) Inhomogeneous electron gas. *Phys Rev* 136:B864–B871
- Kohn W, Sham LJ (1965) Self-consistent equations including exchange and correlation effects. *Phys Rev* 140:A1133–A1137
- Becke AD (1993) Density-functional thermochemistry. III. The role of exact exchange. *J Chem Phys* 98:5648–5652
- Lee C, Yang W, Parr RG (1988) Development of the Colle-Salvetti correlation-energy formula into a functional of the electron density. *Phys Rev B* 37:785–789
- Stephens PJ, Devlin FJ, Chabalowski CF, Frisch MJ (1994) Ab Initio calculation of vibrational absorption and circular dichroism spectra using density functional force fields. *J Phys Chem* 98:11623–11627
- Frisch MJ, Trucks GW, Schlegel HB, Scuseria GE, Robb MA, Cheeseman JR, Zakrzewski VG, Montgomery JA Jr, Stratmann RE, Burant JC, Dapprich S, Millam JM, Daniels AD, Kudin KN, Strain MC, Farkas O, Tomasi J, Barone V, Cossi M, Cammi R, Mennucci B, Pomelli C, Adamo C, Clifford S, Ochterski J, Petersson GA, Ayala PY, Cui Q, Morokuma K, Malick DK,

- Rabuck AD, Raghavachari K, Foresman JB, Cioslowski J, Ortiz JV, Baboul AG, Stefanov BB, Liu G, Liashenko A, Piskorz P, Komaromi I, Gomperts R, Martin RL, Fox DJ, Keith T, Al-Laham MA, Peng CY, Nanayakkara A, Gonzalez C, Challacombe M, Gill PMW, Johnson B, Chen W, Wong WM, Andres JL, Gonzalez C, Head-Gordon M, Replogle ES, Pople JA (2003) Gaussian03, Rev B03. Gaussian Inc, Pittsburgh, PA
31. Foresman JB, Frisch AE (1996) Exploring chemistry with electronic structure methods, 2nd edn. Gaussian Inc, Pittsburgh, PA
 32. Foresman JB, Head-Gordon M, Pople JA, Frisch MJ (1992) Toward a systematic molecular orbital theory for excited states. *J Phys Chem* 96:135–149
 33. Stratmann RE, Scuseria GE, Frisch MJ (1998) An efficient implementation of time-dependent density-functional theory for the calculation of excitation energies of large molecules. *J Chem Phys* 109:8218–8224
 34. Reed AE, Weinhold F (1985) Natural localized molecular orbitals. *J Chem Phys* 83:1736–1740
 35. Reed AE, Curtiss LA, Weinhold F (1988) Intermolecular interactions from a natural bond orbital, donor-acceptor viewpoint. *Chem Rev* 88:899–926
 36. Bader RFW (1990) Atoms in molecules. A quantum theory. Oxford, Clarendon
 37. Politzer P, Truhlar DG (1981) In: Chemical applications of atomic and molecular electrostatic potentials. Plenum Press, New York
 38. Kollman P, McKelvey J, Johansson A, Rothenberg S (1975) Theoretical studies of hydrogen-bonded dimers. Complexes involving HF, H₂O, NH₃, CH₄, H₂S, PH₃, HCN, HNC, HCP, CH₂NH, H₂CS, H₂CO, CH₄, CF₃, H, C₂H₂, C₂H₄, C₆H₆, F- and H₃O⁺. *J Am Chem Soc* 97:955–965
 39. Parr RG, Yang W (1989) Density functional theory of atoms and molecules. Oxford, New York
 40. Parr RG, Yang W (1984) Density functional approach to the frontier-electron theory of chemical reactivity. *J Am Chem Soc* 106:4049–4050
 41. Morell C, Grand A, Toro-Labb A (2005) New dual descriptor for chemical reactivity. *J Phys Chem A* 109:205–212
 42. Walsh AD (1953) The electronic orbitals, shapes, and spectra of polyatomic molecules. Part I. AH₂ molecules. *J Chem Soc* 2260–2266
 43. Walsh AD (1953) The electronic orbitals, shapes, and spectra of polyatomic molecules. Part II. Non-hydride AB₂ and BAC molecules. *J Chem Soc* 2266–2288
 44. Walsh AD (1953) The electronic orbitals, shapes, and spectra of polyatomic molecules. Part IX. Hexatomic molecules: ethylene. *J Chem Soc* 2325–2329
 45. Walsh AD (1946) The electronic orbitals, shapes, and spectra of polyatomic molecules. Part X. A note on the spectrum of benzene. *J Chem Soc* 2330–2331
 46. Wendt M, Weinhold F (2001) NBOView, version 1.1. Theoretical Chemistry Institute, University of Wisconsin, Madison
 47. Kabir M, Mookerjee A, Bhattacharya AK (2004) Structure and stability of copper clusters: a tight-binding molecular dynamics study. *Phys Rev A* 69:043203–043213
 48. Winnerwischer G, Maki AG, Johnson RD (1971) Rotational constants for HCN and DCN. *J Mol Spec* 5:149–158
 49. Puzzarini C, Tarroni R, Palmieri P, Demaison J, Senent ML (1996) Rovibrational energy levels and equilibrium geometry of HCP. *J Chem Phys* 105:3132–3141
 50. Chau FT, Tang YW, Song X (1993) Geometries and molecular properties of phosphaethyne cations. *J Mol Struct (Theochem)* 280:233–237
 51. Ishii S, Ohno K, Kumar V, Kawazoe Y (2003) Breakdown of time-reversal symmetry of photoemission and its inverse in small silicon clusters. *Phys Rev B* 68:195412–195417
 52. Bhattacharya BN, Gordy W (1960) Observation of π stark components in microwave spectroscopy: precision measurements on HCN. *Phys Rev* 119:144–149
 53. Tyler JK (1964) Microwave spectrum of methinophosphide, HCP. *J Chem Phys* 40:1170–1171
 54. Hammer NI, Diri K, Jordan KD, Desfrancois C, Compton RN (2003) Dipole-bound anions of carbonyl, nitrile, and sulfoxide containing molecules. *J Chem Phys* 119:3650–3660
 55. Desfrancois C, Abdoul-Carime H, Schermann JP (1996) Ground-state dipole-bound anions. *Int J Mod Phys B* 10:1339–1395
 56. Compton RN, Hammer NI (2001) Multipole-bound molecular anions. In: Advances in Gas-Phase Ion Chemistry, Elsevier, New York
 57. Jordan KD, Wang F (2003) Theory of dipole-bound anions. *Ann Rev Phys Chem* 54:367–396
 58. Thanikaivelan P, Padmanabhan J, Subramanian V, Ramasami T (2002) Chemical reactivity and selectivity using Fukui functions: basis set and population scheme dependence in the framework of B3LYP theory. *Theor Chem Acc* 107:326–335
 59. GaussView 4.1, Gaussian Inc. 340 Quinipiac St Bldg 40 Wallingford, CT 06492, USA
 60. Cremer D, Kraka E (1984) A description of the chemical-bond in terms of local properties of electron-density and energy. *Croat Chem Acta* 57:1259–1281
 61. Espinosa E, Alkorta I, Elguero J, Molins E (2002) From weak to strong interactions: a comprehensive analysis of the topological and energetic properties of the electron density distribution involving X–H...F–Y systems. *J Chem Phys* 117:5529–5542
 62. Bader RFW, Essen H (1984) The characterization of atomic interactions. *J Chem Phys* 80:1943–1960
 63. Glendening JKB ED, Reed AE, Carpenter JE, Bohmann JA, Morales CM, Weinhold F (2001) NBO 5.0 Program. Madison